DOI: 10.1007/s11099-018-0775-y PHOTOSYNTHETICA 56 (1): 229-235, 2018

Analysis of photosystem II electron transfer with natural PsbA-variants by redox polymer/protein biophotoelectrochemistry

V. HARTMANN[*], A. RUFF[**], W. SCHUHMANN[**], M. RÖGNER[*], and M.M. NOWACZYK[*,+]

Plant Biochemistry, Faculty of Biology and Biotechnology, Ruhr-University Bochum, Universitätsstr. 150, 44780 Bochum, Germany[*]
Analytical Chemistry – Center for Electrochemical Science (CES), Faculty of Chemistry and Biochemistry, Ruhr-University Bochum, Universitätsstr. 150, 44780 Bochum, Germany[**]

Abstract

Redox polymer/protein biophotoelectrochemistry was used to analyse forward electron transfer of isolated PSII complexes with natural PsbA-variants. PsbA1- or PsbA3-PSII was embedded in a redox hydrogel that allows diffusion-free electron transfer to the electrode surface and thus measurement of an immediate photocurrent response. The initial photocurrent density of the electrode is up to ~2-fold higher with PsbA1-PSII under all tested light conditions, the most prominent under high-light [2,300 μmol(photon) m^{-2} s^{-1}] illumination with 5 μA cm^{-2} for PsbA3-PSII and 9.5 μA cm^{-2} for PsbA1-PSII. This indicates more efficient electron transfer in low-light-adapted PsbA1-PSII. In contrast, the photocurrent decays faster in PsbA1-PSII under all tested light conditions, which suggests increased stability of high-light-adapted PsbA3-PSII. These results confirm and extend previous observations that PsbA3-PSII has increased $P680^{+\bullet}/Q_A^{-\bullet}$ charge recombination and thus less efficient photon-to-charge conversion, whereas PsbA1-PSII is optimised for efficient electron transfer with limited stability.

Additional key words: biophotovoltaics; cyanobacteria; D1-protein; hydrogel.

Introduction

Photosystem II (PSII) is a multi-subunit protein complex that catalyses the light-driven water oxidation as the initial step of the photosynthetic electron transfer chain (PET). Cyanobacterial PSII is made up of 17 membrane-integral subunits and 3 extrinsic proteins, which bear 35 chlorophylls (Chl), 2 pheophytins (Phe), 2 hemes, 1 nonheme iron, 2 plastoquinones (Q_A and Q_B), 1 Mn_4CaO_5 cluster, 2 Cl^-, 12 carotenoids, and 25 lipids (Umena *et al.* 2011). Light-induced charge separation at the reaction centre Chls (P680) leads to fast electron transfer (~3 ps) towards the primary acceptor Phe (Holzwarth *et al.* 2006). The resulting cation $P680^+$ oxidises a nearby tyrosine residue which in turn oxidises the Mn_4CaO_5 cluster. This protein-embedded metal cluster stores the oxidizing equivalents, which drive high-efficient water oxidation (Cox and Messinger 2013). On the electron acceptor side, the electron is transferred *via* Q_A to the diffusible two-electron, two-proton mediator Q_B, that is reoxidised by the cytochrome (Cyt)-b_6f membrane protein complex (Baniulis *et al.* 2008), the subsequent electron acceptor within the PET.

PSII operates with high efficiency, in particular, the light-harvesting efficiency (the probability for a photon being absorbed by PSII), the trapping efficiency (the probability for transfer of the excited state to P680 and generation of $P680^*$), and the quantum yield [the probability that generation of $P680^*$ results in formation of $P680^{+\bullet}/Q_A^{-\bullet}$, the first metastable (~1 ms) radical pair] can be close to 100 % under optimal conditions (Dau and Zaharieva 2009). However, in the natural system, forward electron transfer is often limited by overreduction of the

Received 17 July 2017, *accepted* 28 November 2017, *published as online-first* 10 January 2018.
+Corresponding author; email: Marc.M.Nowaczyk@rub.de
Abbreviations: Chl – chlorophyll; Cyt – cytochrome; DCMU – 3-(3,4-dichlorophenyl)-1,1-dimethylurea; LED – light emitting diode; MES – 2-(N-morpholino)ethanesulfonic acid; P680 – reaction centre chlorophylls; PEG-DGE – poly(ethyleneglycol)diglycidylether; PET – photosynthetic electron transfer chain; Phe – pheophytin; P_{Os} – redox-hydrogel; Q – plastoquinone; ROS – reactive oxygen species; β-DM – N-dodecyl-β-D-maltoside.
Acknowledgements: We thank Claudia König and Melanie Völkel for excellent technical assistance. This work was financially supported by the Deutsch–Israelische Projektkooperation (DIP) in the framework of the project "Nanoengineered Optobioelectronics with Biomaterials and Bioinspired Assemblies" and by the Cluster of Excellence RESOLV (EXC 1069) funded by the Deutsche Forschungsgemeinschaft.

plastoquinone pool ("closed" reaction centers) which results in total loss of the converted light energy by charge recombination. Moreover, this process can occur *via* different pathways: (*1*) direct recombination of the $P680^{+\bullet}/Q_A^{-\bullet}$ radical pair, (*2*) repopulation of the $P680^{+\bullet}/Phe^{-\bullet}$ radical pair and recombination *via* the singlet recombination route, or (*3*) formation of P680 triplet state $^3[P680^{+\bullet}/Phe^{-\bullet}]$ and recombination *via* the triplet route. The latter pathway is dangerous, as triplet Chl can easily generate highly reactive singlet oxygen (Krieger-Liszkay *et al.* 2008). Singlet oxygen and other reactive oxygen species (ROS) cause inactivation of PSII by damage of the central D1-protein, which must be replaced continuously (Nixon *et al.* 2010). Triplet Chl formation can be avoided by adaptation of the Phe/Q_A redox potentials. A larger energy gap between the two redox centres would prevent repopulation of the $Phe^{-\bullet}/Q_A$ state as well as subsequent formation of $^3[P680^{+\bullet}/Phe^{-\bullet}]$. Moreover, direct recombination of $P680^{+\bullet}/Q_A^{-\bullet}$ to P680/Q_A would be more likely when the midpoint potential of Q_A/Q_A^- is increased (Sugiura and Boussac 2014). These conclusions point towards the fundamental dilemma: charge recombination lowers the efficiency of the process, specifically under low-light conditions when $Q_B^{-\bullet}$ needs to be stabilised until the second electron is provided.

However, cyanobacteria have solved this problem by flexible adaptation of the Phe/Q_A redox potentials, which is a fascinating example how biological systems can further optimise a catalyst by dynamic variation of its properties at the molecular level (Sander *et al*. 2010, Sugiura *et al*. 2010, 2014). They encode different variants of the D1 protein that are differentially expressed depending on environmental conditions (Schaefer and Golden 1989, Clarke *et al*. 1993, Tichý *et al*. 2003, Sicora *et al*. 2006). The thermophilic cyanobacterium *Thermosynechococcus elongatus* changes between three D1 variants (PsbA1, PsbA2, and PsbA3); while PsbA1 is expressed under standard (low-light) growth conditions, transcription of PsbA3 is quickly induced under high-light conditions (Kós *et al.* 2008) and microaerobic cultivation seems to trigger PsbA2 expression (Sugiura *et al.* 2012). Main difference between the low-light and high-light-adapted D1 copy is the exchange of glutamate (PsbA1) to glutamine (PsbA3) at position 130, which causes differences in the hydrogen bond network of the adjacent Phe (Ogami *et al.* 2012). In total 21 of 344 amino acid residues are changed between the two D1 copies, thus shifting the midpoint potential of Q_A/Q_A^- by ~41 mV from –124 mV (PsbA1) to –83 mV (PsbA3); also, this extends the energy gap between $Phe^{-\bullet}/Q_A$ and $Phe/Q_A^{-\bullet}$ by 24 mV (Sugiura *et al.* 2014). The physiological consequences of this adaptation have been studied for example by recombinant expression of the cyanobacterial D1 copies PsbA1 and PsbA3 in the green algae *Chlamydomonas reinhardtii* (Vinyard *et al.* 2013, 2014). The strain with the low-light-adapted PsbA1 variant could accumulate 12% more biomass under low-light conditions compared to the strain with the high-light-adapted PsbA3 copy. Plants and algae naturally contain only the high-light-adapted PsbA3 variant, which may indicate that PsbA1 is a special cyanobacterial feature that allows growth under very low light intensities (Sander *et al.* 2010).

The high efficiency of PSII has stimulated the development of semi-artificial biohybrid photovoltaic assemblies. First electrochemical experiments were carried out by PSII-containing layered modifications and diffusible mediators as electron carriers (Trammell *et al.* 2004, Badura *et al.* 2006, Yehezkeli *et al.* 2013). Recently scientific progress focused on the adaption of redox-active hydrogels to overcome diffusion-dependent electron transport (Badura *et al.* 2008, Yehezkeli *et al.* 2012, Kothe *et al.* 2013, Hartmann *et al.* 2014), with the midpoint potential of the designed hydrogels being adapted to the redox potential of Q_B at the acceptor site of PSII. This allows the setup of bias-free bio-photovoltaic devices. Further improvements in current density can be achieved by optimization of the electrode material (Kato *et al.* 2012a, Sokol *et al.* 2016). Three-dimensional structures allow a higher PSII loading and decrease the distance to the electrode surface by porous electrode materials.

We here introduce redox polymer/protein biophotoelectrochemistry as a versatile tool for the characterisation of isolated PSII complexes with natural D1 variants. The electrochemical setup provides diffusion-free electron transfer from PSII with either PsbA1 or PsbA3 *via* redox-active hydrogels towards the electrode that can be directly monitored by measurement of the corresponding photocurrent.

Materials and methods

Chemicals used were 2-(N-morpholino)ethanesulfonic acid (MES; ≥99%), KCl (≥99%), $MgCl_2$ anhydrous (≥98%), and $CaCl_2$ anhydrous (≥93%) from *Sigma-Aldrich* (Taufkirchen, Germany), poly(ethyleneglycol)diglycidyl-ether (PEG-DGE) from *Polysciences* (Warrington, USA), and N-dodecyl-β-D-maltoside (β-DM) from *Glycon Biochemicals* (Luckenwalde, Germany).

Protein purification: PSII was isolated from the thermophilic cyanobacterium *Thermosynechococcus elongatus*. Intact dimeric PSII complexes were isolated according to Kuhl *et al.* (2000), with PsbA1-PSII originating from the corresponding Δ*psbA3* mutant and PsbA3-PSII from the Δ*psbA1A2* mutant. Construction of the knockout-mutants was reported previously and the amount of PsbA2 in the PsbA1-PSII preparation was shown to be below detection limit (Sander *et al.* 2010).

Synthesis of the redox hydrogel P_{Os}: The synthesis of polymer P_{Os} (poly(1-vinylimidazole-co-allylamine)-

[Os(II)(bpy)$_2$Cl]Cl) was reported earlier (Sokol *et al.* 2016). The Os-precursor Os(bpy)$_2$Cl$_2$ (bpy = 2,2'-bipyridine) was prepared according to Habermüller *et al.* (2000).

Electrode modification: Electrodes were modified using PSII variants immobilized in the redox-hydrogel P_{Os} as follows. A 5-µl droplet containing 5 mg(P_{Os}) mL^{-1}, 0.02 mg mL^{-1} of PEG-DGE dissolved in distilled water and 1 mg mL^{-1} of PSII [stock 6.7 mg(Chl) mL^{-1}] in buffer solution [50 mM MES, pH 6.5, 10 mM $MgCl_2$, 10 mM $CaCl_2$, and 0.03% (w/v) β-DM] was deposited on a 2-mm Au-disk electrode. The electrodes were kept in the dark at 4°C for 3 h. Prior to use, the electrodes were washed shortly with buffer solution to remove loosely bound compounds.

Electrochemical measurements were performed using an *AUTOLAB PGSTAT12* potentiostat/galvanostat upon illumination with a light emitting diode (LED) *(FAT-685-40, Roithner,* Vienna, Austria) with a maximum power output of 2,300 µmol(photon) m^{-2} s^{-1} at 685 nm. The light intensity was adapted by changing the applied power on LED with the computer-based control unit *PXI-1033* with a DC precision power supply module *PXI-4110* (*National Instruments Germany GmbH,* Munich, Germany).

Chronoamperometric measurements and cyclic voltammetry were carried out in 5 mL of buffer solution [50 mM MES pH 6.5, 10 mM $MgCl_2$, 10 mM $CaCl_2$, 100 mM KCl, and 0.03% (w/v) β-DM] with a platinum wire (1 mm diameter) as a counter electrode and a self-made Ag/AgCl (3.5 M KCl) reference electrode (East and del Valle 2000). In chronoamperometric measurements, a potential of +400 mV was applied for 30 s prior to each measurement to oxidize the polymer-bound Os-complexes.

Equations:
The activity decrease over time is given by

$$p = \frac{[B(0)-B(t)]/t}{B(0)*100} \quad (1)$$

where p is the percentage of decrease over time [%], B(0) is photocurrent after 200 s of illumination [µA cm^{-2}], B(t) is photocurrent after time t [µA cm^{-2}], and t is time [s].

The decrease factor is given by $q = 1 - \frac{p}{100}$ (2)

where q is the decrease factor and p is the percentage of decrease over time [%].

The half-life time is given by $T_{1/2} = \frac{\ln(0.5)}{\ln(q)} /60$ (3)

where $T_{1/2}$ represents the half-life time [min] and q is the decrease factor.

The IPCE value represents the external quantum efficiency and is given by $IPCE = \frac{I_{photo}/e}{P_i/\gamma_{685}} \times 100$ (4)

where IPCE stands for incident photon-to-electron conversion efficiency [%], I_{photo} is the calculated photocurrent at the beginning of a measurement [A cm^{-2}], e represents the elementary charge of one electron (~1.6022 × 10^{-19} C), P_i is the detected light intensity of LED on electrode surface [W cm^{-2}], and γ_{685} is the energy of one photon at a wavelength of 685 nm (~2.8905 × 10^{-19} W).

Results and discussion

We have previously analysed isolated PsbA1- and PsbA3-PSII complexes by delayed as well as flash-induced fluorescence spectroscopy and thermoluminescence measurements. They all indicated, that recombination of the $P680^{+\bullet}/Q_A^{-\bullet}$ radical pair is more likely in PsbA3-PSII (Sander *et al.* 2010). However, oxygen-evolving activity measurements under high light intensities showed no difference between the complexes in our analysis and correlate with previous studies (Sander *et al.* 2010). PsbA1-PSII shows an oxygen-evolution rate of 2,950 ± 270 µmol(O_2) µg^{-1}(Chl) h^{-1} and PsbA3-PSII a rate of 2,850 ± 170 µmol(O_2) µg^{-1}(Chl) h^{-1}. Contrary, other studies showed a ~2-fold increase of the oxygen-evolution rate of PsbA3-PSII, which was claimed to be attributed to a faster Q_BH_2 exchange rate (Kato *et al.* 2012b, Sugiura and Boussac 2014). In order to establish a more direct measurement of PSII electron transfer *in vitro*, which is independent of diffusion-limited electron mediators, we determined the photocurrent of redox-hydrogel embedded PsbA1- and PsbA3-PSII under various light conditions.

For this purpose, electrodes were prepared by drop coating with a mixture of PSII, osmium complex-modified polymers, and cross-linker that ensures stable surface modifications. However, the loss of a weakly immobilised PSII/polymer fraction may contribute to a time-dependent decrease of the photocurrent being unrelated to the PSII activity. In order to exclude this side-effect during chronoamperometric measurements, we examined the hydrogel stability by long-term cyclic voltammetry (Fig. 1). In this case, the loss of redox-active groups at the electrode surface can be monitored by the decrease of the peak current for the Os^{2+} oxidation reaction, showing a significant loss of redox-active centres within the first 200 s. However, after this initial drop, the remaining hydrogel film is very stable showing no significant changes for >30 min.

Moreover, rapid inactivation of poorly connected PSII complexes contributes to the initial drop in photocurrent. In this case, PSII remains immobilised at the electrode surface, while a subfraction is quickly inactivated due to limited electron transfer towards the redox hydrogel. This can be explained by random distribution of PSII complexes and polymer-bound redox groups within the final polymer film. PSII being in suboptimal distance and orientation to the closest redox center of the polymer is

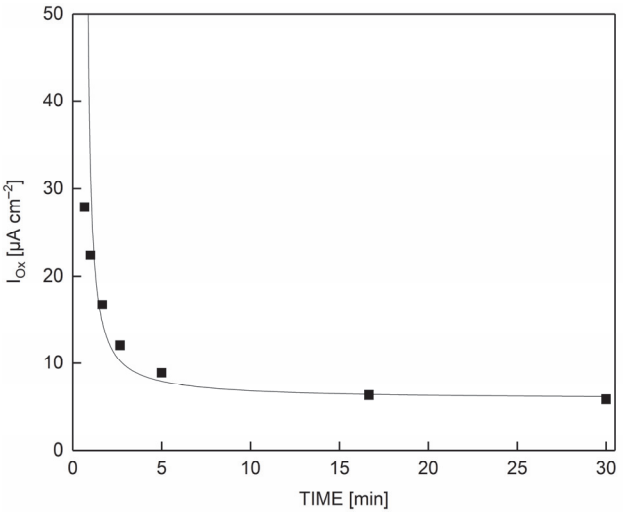

Fig. 1. Observed maximum Os^{2+} oxidation peak current obtained by successive cyclic voltammetry plotted *vs*. time. Au-electrode modified with PSII, P_{Os}, and cross-linker PEG-DGE in the potential range from –100 mV to +400 mV *vs*. Ag/AgCl/3.5 M KCl at room temperature, in darkness and a scan rate of 50 mV s^{-1}. Analysis of a total number of 90 cycles, followed by logarithmical curve fitting to the oxidation current at given cycles.

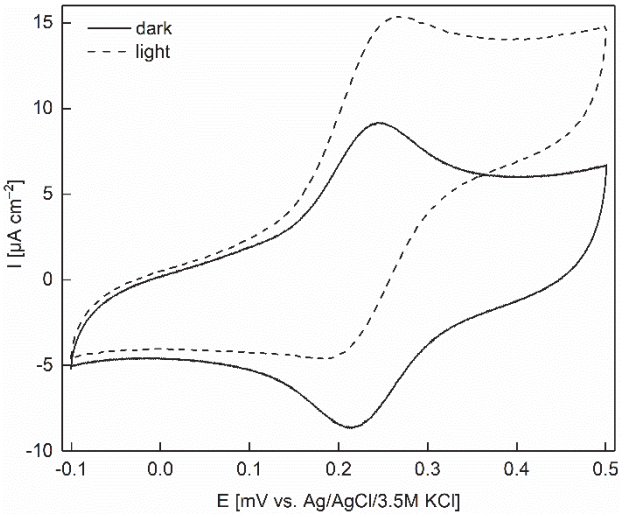

Fig. 2. Cyclic voltammogram of a redox polymer/PS2 modified electrode in darkness (*solid line*) and under illumination with 2,300 µmol(photon) m^{-2} s^{-1} at 685 nm wavelength (*dashed line*) in a range from –100 mV to +500 mV *vs*. Ag/AgCl/3.5M KCl with a scan rate of 50 mV s^{-1}.

damaged and inactivated by ROS formation within the first 200 s of illumination (Vöpel *et al.* 2015). The catalytic function of the remaining PSII complexes is not affected by the preincubation time and can be monitored by cyclic voltammetry in darkness followed by illumination (Fig. 2) (Badura *et al.* 2006, 2008). The positive shift at the oxidative reversal point indicates the rise of transferred electrons by PSII. This catalytic current can be followed during illumination by chronoamperometric measurements at a fixed applied potential.

Using this setup, we compared photo-induced current densities of electrodes with redox-polymer embedded PsbA1-PSII and PsbA3-PSII under different light intensities. Fig. 3 shows as an example of a photocurrent density transient of PsbA1-PSII. The sample was illuminated with red light (685 nm) at high intensity [860 µmol(photon) m^{-2} s^{-1}] in a 30-s light-dark cycle to avoid baseline shift (Sokol *et al.* 2016). As expected, a two-phase decay kinetic was observed, with the first fast phase being attributed to the initial instability of the polymer film and a rapid inactivation of poorly connected PSII complexes. The second phase (>200 s of illumination) reflects slower light-induced inactivation of the remaining PSII complexes.

Initial photocurrent densities were recorded after 200 s of illumination (400 s of measurement) with samples being illuminated under low [65 and 130 µmol(photon) m^{-2} s^{-1}], intermediate [300 µmol(photon) m^{-2} s^{-1}] and high-light intensities [860 and 2,300 µmol(photon) m^{-2} s^{-1}]. The determined photocurrent densities being a direct indicator for the forward electron transfer rate, are significantly higher for PsbA1-PSII at almost all light intensities (Fig. 4). In particular, under high-light conditions [2,300 µmol(photon) m^{-2} s^{-1}] the current density of PsbA1-PSII (9.5 µA cm^{-2}) is ~2-fold higher compared to PsbA3-PSII (5 µA cm^{-2}). To our knowledge, this is the first direct evidence for more efficient forward electron transfer in PsbA1-PSII under optimal conditions. An explanation may be the more negative midpoint potential of Phe and Q_A in PsbA1 (Sugiura *et al.* 2014) generating a higher driving force for electron transfer towards the acceptor and minimizing losses by charge recombination. Although presently the exact electron pathway from PSII to the

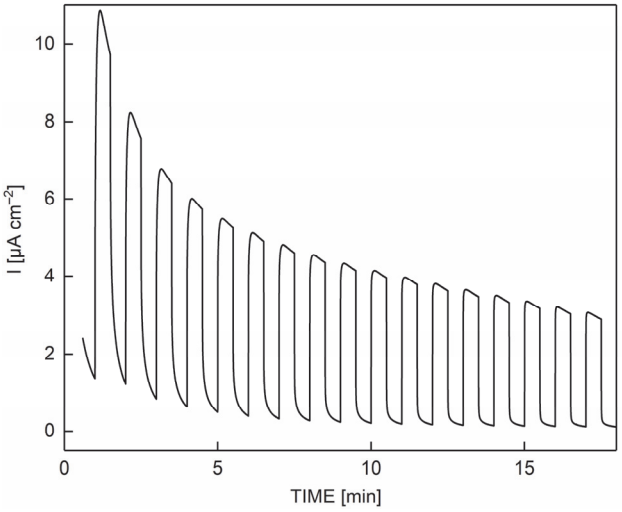

Fig. 3. Photocurrent density of electrodes with redox-hydrogel embedded PSII: Chopped illumination (30-s light–dark cycle) at 685 nm at an intensity of 860 µmol(photon) m^{-2} s^{-1}. A potential of +400 mV *vs*. Ag/AgCl/3.5 M KCl was applied.

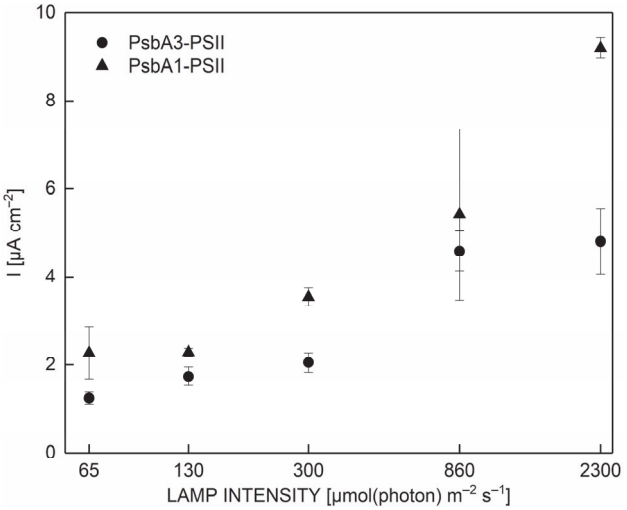

Fig. 4. Observed photo-induced current density of PsbA3-PSII (*circles*) and PsbA1-PSII (*triangles*) at various light intensities at 685 nm. A potential of +400 mV *vs*. Ag/AgCl/3.5 M KCl was applied during the measurement and currents were determined 200 s after start of illumination (n = 3–5).

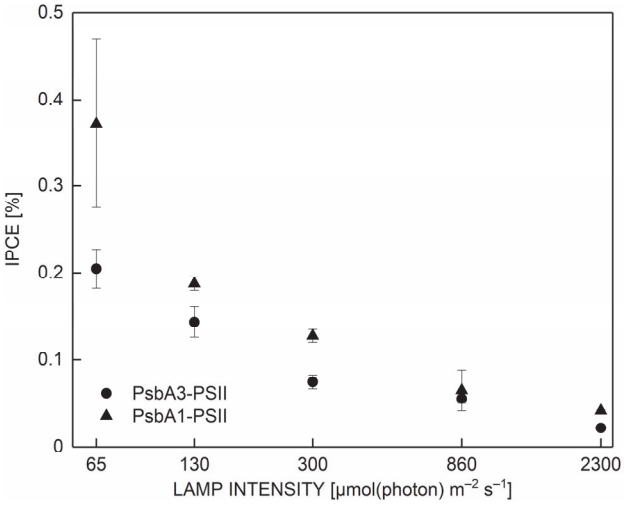

Fig. 5. Incident photon-to-electron conversion efficiency (IPCE) of PsbA3-PSII (circles) and PsbA1-PSII (triangles) under various light intensities at an illumination wavelength of 685 nm (n = 3–5).

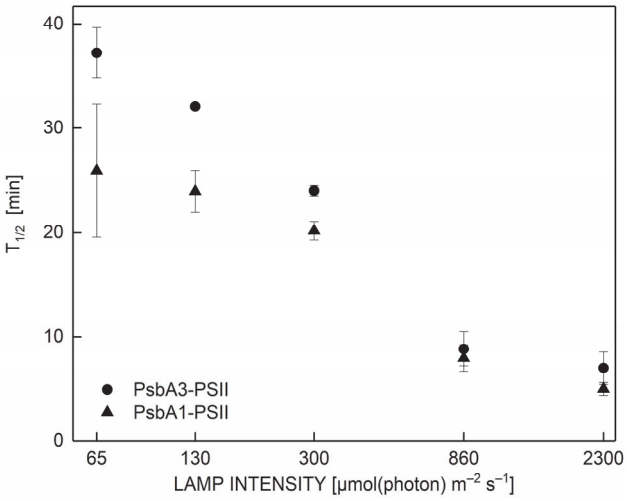

Fig. 6. Calculated half-life time for PsbA3-PSII (circles) and PsbA1-PSII (triangles) under various light intensities at an illumination wavelength of 685 nm (n = 3–5).

hydrogel is unknown, a direct transfer from $Q_A^{-\bullet}$ or $Q_B^{-\bullet}$ to the polymer bound Os-complexes seems likely. This is at least indicated by only partial inhibition (~80%) of the photocurrent after addition of the PSII inhibitor DCMU (Figs. 1S, 2S; *supplements available online*). However, as binding of DCMU shifts also the redox potential of Q_A more positive (Krieger-Liszkay and Rutherford 1998) and access to the binding site might be limited within the cross-linked hydrogel, further investigations are necessary to clarify the exact pathway.

The observed light-dependent photocurrent densities were further used to calculate the incident photon-to-electron conversion efficiency (IPCE) that is usually used to evaluate the quantum yield of solar cells (Eq. 4). PsbA1-PSII shows a higher quantum yield than PsbA3-PSII, especially under low-light illumination (Fig. 5), which is also in agreement with its physiological role. However, under high-light conditions of 2,300 µmol(photon) m^{-2} s^{-1}, only a very low IPCE of 0.041 ± 0.001% (PsbA1-PSII) and 0.022 ± 0.003% (PsbA3-PSII) was detected (Fig. 4). This may be due to the relative thin layer (~µm) of polymer-embedded photosystems that limits the amount of PSII per illuminated area.

In contrast to our results, it has been previously reported that high-light-adapted PsbA3-PSII yields a higher O_2 quantum yield and also a higher turnover frequency when calculated based on oxygen-evolution rates (Kato *et al.* 2012b, Vinyard *et al.* 2013, Sugiura and Boussac 2014). We explain this observation by different inactivation rates of PsbA1- and PsbA3-PSII during O_2 evolution measurements, which compensate differences in electron transfer rates. In order to test this hypothesis, we calculated the PsbA1- and PsbA3-PSII half-life times from the photocurrent density transients (Fig. 3) at different light intensities using Eqs. 1–3 (Fig. 6).

In this case, PsbA3-PSII shows a higher stability than PsbA1-PSII under all tested light intensities (Fig. 6), which is in agreement with the special function of PsbA3 and might explain the higher oxygen-evolution rates of PsbA3-PSII (Sugiura and Boussac 2014). The largest difference is visible at the lowest tested light intensity of 65 µmol (photon) m^{-2} s^{-1}, with a half-life time of 37 ± 2 min for PsbA3-PSII and 26 ± 6 min for PsbA1-PSII (Fig. 6). Above 860 µmol(photon) m^{-2} s^{-1}, increasing the substrate light to 2,300 µmol(photon) m^{-2} s^{-1} does not seriously affect the half-life time for both complexes, indicating a saturated protection mechanism in PsbA3-PSII under these light conditions.

In conclusion, we have shown that direct measurement

of PSII electron transfer by the determination of photocurrent densities is a valuable tool to analyse adaptation of PSII function in natural PsbA variants. Our setup is optimised for diffusion-free forward electron transfer from PSII towards the electrode, which results in a direct link between PSII electron transfer and photocurrent response. This system allows to differentiate between PSII activity and inactivation, two processes, which are closely connected and which are particularly important for the analysis of PSII complexes with adjusted electron transfer like PsbA1- and PsbA3-PSII. Future work should focus on the analysis and further engineering of the PSII-redox-polymer interface by the development of novel redox-polymers (Hartmann *et al.* 2014) and tailor-made adaptation of PSII by site-directed mutagenesis.

References

Badura A., Esper B., Ataka K. *et al.*: Light-driven water splitting for (bio-)hydrogen production. Photosystem 2 as the central part of a bioelectrochemical device. – Photochem. Photobiol. **82**: 1385-1390, 2006.

Badura A., Guschin D., Esper B. *et al.*: Photo-induced electron transfer between Photosystem 2 *via* cross-linked redox hydrogels. – Electroanalysis **20**: 1043-1047, 2008.

Baniulis D., Yamashita E., Zhang H. *et al.*: Structure-function of the cytochrome b_6f complex. – Photochem. Photobiol. **84**: 1349-1358, 2008.

Clarke A.K., Hurry V.M., Gustafsson P., Oquist G.: Two functionally distinct forms of the photosystem II reaction-center protein D1 in the cyanobacterium *Synechococcus sp.* PCC 7942. – P. Natl. Acad. Sci. USA **90**: 11985-11989, 1993.

Cox N., Messinger J.: Reflections on substrate water and dioxygen formation. – BBA-Bioenergetics **1827**: 1020-1030, 2013.

Dau H., Zaharieva I.: Principles, efficiency, and blueprint character of solar-energy conversion in photosynthetic water oxidation. – Acc. Chem. Res. **42**: 1861-1870, 2009

East G.A., del Valle M.A.: Easy-to-make Ag/AgCl reference electrode. – J. Chem. Educ. **77**: 97, 2000.

Habermüller K., Ramanavicius A., Laurinavicius V., Schuhmann W.: An oxygen-insensitive reagentless glucose biosensor based on osmium-complex modified polypyrrole. – Electroanalysis **12**: 1383-1389, 2000.

Hartmann V., Kothe T., Pöller S. *et al.*: Redox hydrogels with adjusted redox potential for improved efficiency in Z-scheme inspired biophotovoltaic cells. – Phys. Chem. Chem. Phys. **16**: 11936-11941, 2014.

Holzwarth A.R., Müller M.G., Reus M. *et al.*: Kinetics and mechanism of electron transfer in intact photosystem II and in the isolated reaction center. Pheophytin is the primary electron acceptor. – P. Natl. Acad. Sci. USA **103**: 6895-6900, 2006.

Kato M., Cardona T., Rutherford A.W., Reisner E.: Photoelectrochemical water oxidation with photosystem II integrated in a mesoporous indium-tin oxide electrode. – J. Am. Chem. Soc. **134**: 8332-8335, 2012a.

Kato Y., Shibamoto T., Yamamoto S. *et al.*: Influence of the PsbA1/PsbA3, Ca^{2+}/Sr^{2+} and Cl^-/Br^- exchanges on the redox potential of the primary quinone Q_A in Photosystem II from *Thermosynechococcus elongatus* as revealed by spectroelectrochemistry. – BBA-Bioenergetics **1817**: 1998-2004, 2012b.

Kós P.B., Deák Z., Cheregi O., Vass I.: Differential regulation of *psbA* and *psbD* gene expression, and the role of the different D1 protein copies in the cyanobacterium *Thermosynechococcus elongatus* BP-1. – Biochim. Biophys. Acta **1777**: 74-83, 2008.

Kothe T., Plumeré N., Badura A. *et al.*: Combination of a photosystem 1-based photocathode and a photosystem 2-based photoanode to a Z-scheme mimic for biophotovoltaic applications. – Angew. Chem. Int. Edit. **52**: 14233-14236, 2013.

Krieger-Liszkay A., Fufezan C., Trebst A.: Singlet oxygen production in photosystem II and related protection mechanism. – Photosynth. Res. **98**: 551-564, 2008.

Krieger-Liszkay A., Rutherford A.W.: Influence of herbicide binding on the redox potential of the quinone acceptor in photosystem II: Relevance to photodamage and phytotoxicity. – Biochemistry **37**: 17339-17344, 1998.

Kuhl H., Kruip J., Seidler A. *et al.*: Towards structural determination of the water-splitting enzyme. Purification, crystallization, and preliminary crystallographic studies of photosystem II from a thermophilic cyanobacterium. – J. Biol. Chem. **275**: 20652-20659, 2000.

Nixon P.J., Michoux F., Yu J. *et al.*: Recent advances in understanding the assembly and repair of photosystem II. – Ann. Bot.-London **106**: 1-16, 2010.

Ogami S., Boussac A., Sugiura M.: Deactivation processes in PsbA1-Photosystem II and PsbA3-Photosystem II under photoinhibitory conditions in the cyanobacterium *Thermosynechococcus elongatus*. – Biochim. Biophys. Acta **1817**: 1322-1330, 2012.

Sander J., Nowaczyk M., Buchta J. *et al.*: Functional characterization and quantification of the alternative PsbA copies in *Thermosynechococcus elongatus* and their role in photoprotection. – J. Biol. Chem. **285**: 29851-29856, 2010.

Schaefer M.R., Golden S.S.: Differential expression of members of a cyanobacterial *psbA* gene family in response to light. – J. Bacteriol. **171**: 3973-3981, 1989.

Sicora C.I., Appleton S.E., Brown C.M. *et al.*: Cyanobacterial *psbA* families in *Anabaena* and *Synechocystis* encode trace, constitutive and UVB-induced D1 isoforms. – BBA-Bioenergetics **1757**: 47-56, 2006.

Sokol K.P., Mersch D., Hartmann V. *et al.*: Rational wiring of photosystem II to hierarchical indium tin oxide electrodes using redox polymers. – Energ. Environ. Sci. **9**: 3698-3709, 2016.

Sugiura M., Azami C., Koyama K. *et al.*: Modification of the pheophytin redox potential in *Thermosynechococcus elongatus* Photosystem II with PsbA3 as D1. – BBA-Bioenergetics **1837**: 139-148, 2014.

Sugiura M., Boussac A.: Some Photosystem II properties depending on the D1 protein variants in *Thermosynechococcus elongatus*. – BBA-Bioenergetics **1837**: 1427-1434, 2014.

Sugiura M., Kato Y., Takahashi R. *et al.*: Energetics in photosystem II from *Thermosynechococcus elongatus* with a D1 protein encoded by either the *psbA1* or *psbA3* gene. – Biochim. Biophys. Acta **1797**: 1491-1499, 2010.

Sugiura M., Ogami S., Kusumi M. *et al.*: Environment of Tyr_Z in photosystem II from *Thermosynechococcus elongatus* in which

PsbA2 is the D1 protein. – J. Biol. Chem. **287**: 13336-13347, 2012.

Tichý M., Lupínková L., Sicora C. *et al.*: *Synechocystis* 6803 mutants expressing distinct forms of the Photosystem II D1 protein from *Synechococcus* 7942. Relationship between the *psbA* coding region and sensitivity to visible and UV-B radiation. – BBA-Bioenergetics **1605**: 55-66, 2003.

Trammell S.A., Wang L., Zullo J.M. *et al.*: Orientated binding of photosynthetic reaction centers on gold using Ni-NTA self-assembled monolayers. – Biosens. Bioelectron. **19**: 1649-1655, 2004.

Umena Y., Kawakami K., Shen J.-R., Kamiya N.: Crystal structure of oxygen-evolving photosystem II at a resolution of 1.9 Å. – Nature **473**: 55-60, 2011.

Vinyard D.J., Gimpel J., Ananyev G.M. *et al.*: Natural variants of photosystem II subunit D1 tune photochemical fitness to solar intensity. – J. Biol. Chem. **288**: 5451-5462, 2013.

Vinyard D.J., Gimpel J., Ananyev G.M. *et al.*: Engineered Photosystem II reaction centers optimize photochemistry versus photoprotection at different solar intensities. – J. Am. Chem. Soc. **136**: 4048-4055, 2014.

Vöpel T., Ning Saw E., Hartmann V. *et al.*: Simultaneous measurements of photocurrents and H_2O_2 evolution from solvent exposed photosystem 2 complexes. – Biointerphases **11**: 19001, 2015.

Yehezkeli O., Tel-Vered R., Michaeli D. *et al.*: Photosystem I (PSI)/Photosystem II (PSII)-based photo-bioelectrochemical cells revealing directional generation of photocurrents. – Small **9**: 2970-2978, 2013.

Yehezkeli O., Tel-Vered R., Wasserman J. *et al.*: Integrated photosystem II-based photo-bioelectrochemical cells. – Nat. Commun. **3**: 742, 2012.